Design Sensitivity of a Tensegrity Model of a Tissue

Eligiusz Postek

Department of Computational Science, Institute of Fundamental Technological Research of the Polish Academy of Sciences
ul. Pawińskiego 5B, 02-106 Warsaw, Poland
e-mail:ewpostek@gmail.com

Abstract

The design sensitivity algorithm for visco-elastic tensegrity structures is presented. We adopt Updated Lagrangian formulation. We have possibility of grouping of the design variables what is particularly useful in the case of hierarchical structures. In our case, the structure is the tissue built of elementary cells. The design sensitivity procedure is implemented with parallel solver.

Keywords: computational biology, tensegrity structures, design sensitivity

1. Introduction

The cytoskeleton (CSK) can be modelled as a tensegrity structure, Ref. [1]. The role of the CSK is continuously discovered. The mechanical environment is very important to the cells behaviour. We will cite here, Ref. [8] "*Change the mechanical stresses on cancer cells and they can start to behave more like healthy ones*". This is the statement that the mechanical actions affect the living organisms from the level of entire body to the level of the cell and below. The displacements and stresses are changing in the biological materials continuously due to the growth, division and death of the cells, Ref. [6].

The cells undergo different kind of signals which "tells" them to grow, divide, die and reorganize their internal structure (motility phenomenon). The signals can be of electrical, mechanical, thermal, chemical or even unknown nature. This constitutes the agent based models of the tissue, Ref. [9].

The described model, program and the theory will become elements of an agent based system, Ref. [7]. However, this is beyond the scope of the presentation.

2. Methodology, mechanical model

[i]The elementary cell consists of nucleus, actins, microtubules, membrane and collagen. We can see it under the laser confocal microscope, Fig. 1.

We will deal with the mechanical model of the cytoskeleton. The cytoskeleton consists of actins and microtubules. The actins act as tendons and the microtubules act as compressed struts. They build the tensegrity structure of the cell. The observed behaviour of the elementary cells is viscoelastic. They are pre-stressed and keep approximately their volume when deformed and they stiffen when undergo tension.

These conditions are fulfilled by the elementary icosahedron based tensegrity structure, Fig. 2. We deal with the elementary cell model with equivalent actins and microtubules. We adopted the following data, namely, height of the cell 64 μm, cross-sectional areas of the tendons (filaments) 10nm^2, cross-sectional areas of the struts (microtubules) 190 nm^2, Young's moduli of the tendons 2.6GPa and the struts 1.2GPa, initial prestressing forces 20 nN, maximum loading 0.1N, relaxation time 1.0 sec, G_i/G_o ratio 0.91 (case A) and 0.1 (case B). We may note certain effect of the imperfect position of the nodes and higher stiffening effect for higher G_i/G_o ratios (case A).

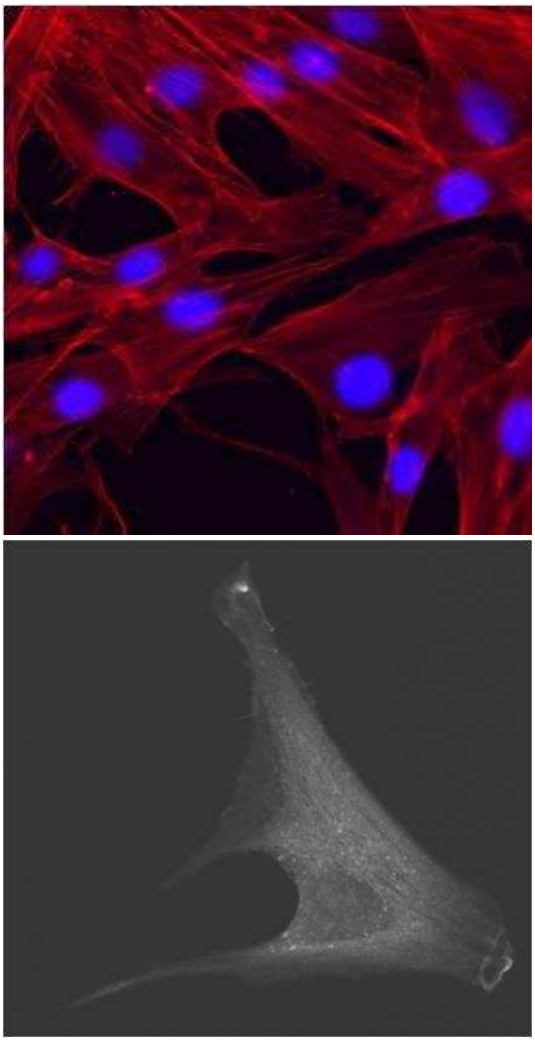

(a) (b)

Figure 1: Human dermal fibroplasts; a) group of cells with nuclei b) cross-section with enhanced actins

The inherent feature of our model is the design sensitivity analysis, Ref. [4, 6]. The displacements and stresses fields are sensitive to the different design parameters, for example, the geometrical parameters like lengths of the actins and

*The parallel version of the program was prepared during the research visit in the High Performance Computing Centre (HLRS) and in the Institute of Materials Testing, Materials Science and Strength of Materials (IMWF) in the University of Stuttgart.
We thank to the Engineering and Physical Research Council, UK for the support under the grant "The Epitheliome: computational modelling of epithelial tissue", GR/S62321/01

microtubules, their cross-sectional areas, constitutive parameters like Young's modulus, relaxation time and shape parameters. The design parameters can be grouped into clusters representing the cells and into groups of clusters. This gives information about the influence of cells, their elements and groups of cells. In fact, observing the derivatives we obtain an additional tool to evaluate the effects of the mechanotransduction. Therefore, we postulate that the design sensitivity analysis should be the inherent feature of the analysis of cell assemblies.

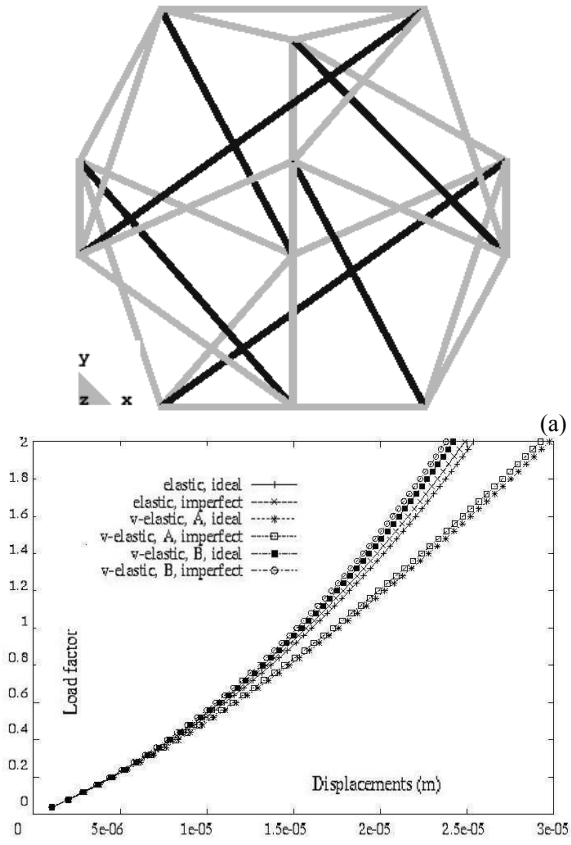

Figure 2: Elementary tensegrity cell; a) geometry, struts under compression – blue and tendons under tension – yellow b) stiffening effect of the tensioned cell, load versus displacement.

3. Mathematical formulation

We adopt the incremental formulation in the Updated Lagrangian frame. The influence of initial stress is exposed via including of the geometrical stiffness matrix.

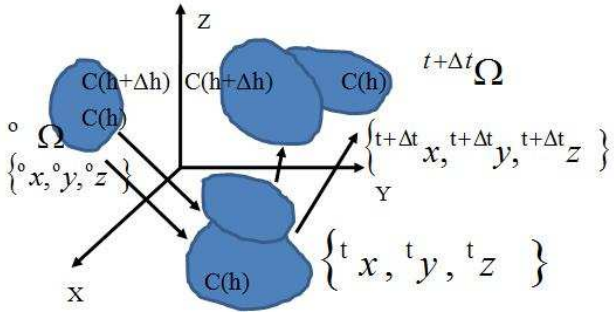

Figure 3: Configurations of the considered body motion.

The general idea of the direct differentiation method is shown in Fig. 3. There are given the initial, intermediate and the predicted configurations. The design parameters of the structure are perturbed at the beginning of its motion and the path of motion of the perturbed structure differs from the ideal one.

The performance functional valid on the body Ω and its boundary $\partial\Omega_\sigma$ depending on displacements $\mathbf{q}$, stresses $\mathbf{S}$ and design parameter h is of the form

$$ {}^{t+\Delta t}_{t}\Phi = \int_{\Omega^t} {}^{t+\Delta t}_{t}G(\mathbf{S},\mathbf{q},h)d\Omega^t + \int_{\partial\Omega^t_\sigma} {}^{t+\Delta t}_{t}g(\mathbf{q},h)d\left(\partial\Omega^t_\sigma\right) \tag{1} $$

Our goal is to find the derivative of the functional with respect to the design variable h at time $t+\Delta t$.

The total potential energy of the nonlinear viscous-elastic system is of the form

$$ \begin{aligned} \Pi = \int_{\Omega^o} \frac{1}{2} {}^{t+\Delta t}_{o}\mathbf{S}\cdot {}^{t+\Delta t}_{o}\mathbf{E}\, d\Omega^o - \int_{\Omega^o} {}^{t+\Delta t}\mathbf{f}\, {}^{t+\Delta t}\mathbf{u}\, d\Omega^o \\ - \int_{\Omega^t_\sigma} {}^{t+\Delta t}\mathbf{t}\, {}^{t+\Delta t}\mathbf{u} d\left(\partial\Omega^t_\sigma\right) \end{aligned} \tag{2} $$

where $\mathbf{S}$ and $\mathbf{E}$ are the II Piola-Kirchhof stress tensor and Green Lagrange strain tensor, $\mathbf{f}$, $\mathbf{t}$ and $\mathbf{u}=\{u,v,w\}$ are body forces, boundary tractions and displacements. All of the values are determined at time $t+\Delta t$ in the initial configuration o. In the spirit of the UL approach we need to transform the equation to the configuration t. Taking the variation of the Eqn. (1) we get the virtual work equation of the form

$$ \begin{aligned} \delta\Pi = \int_{\Omega^o} {}^{t+\Delta t}_{o}\mathbf{S}\cdot\delta\, {}^{t+\Delta t}_{o}\mathbf{E}\, d\Omega^o - \int_{\Omega^o} {}^{t+\Delta t}\mathbf{f}\ \delta\, {}^{t+\Delta t}\mathbf{u}\, d\Omega^o \\ - \int_{\partial\Omega^o_\sigma} {}^{t+\Delta t}\mathbf{t}\,\delta\, {}^{t+\Delta t}\mathbf{u}\, d\left(\partial\Omega^o_\sigma\right) \end{aligned} \tag{3} $$

Exploiting the following relations, Ref [5]

$$ {}^{t+\Delta t}_{0}\mathbf{S} = \frac{\rho}{\rho_0} {}^{t+\Delta t}_{t}\mathbf{S}, \quad {}^{t+\Delta t}_{0}\mathbf{E} = \frac{\rho}{\rho_0} {}^{t+\Delta t}_{t}\mathbf{E}, \quad \rho d\Omega^t = \rho_0 d\Omega^0 \tag{4} $$

we transform the virtual work equation, Eqn. (2), from the reference configuration at time 0 to the reference configuration at time t. The equation reads

$$ \begin{aligned} \int_{\Omega^t} {}^{t+\Delta t}_{t}\mathbf{S}\cdot\delta\, {}^{t+\Delta t}_{t}\mathbf{E} d\Omega^t = \int_{\Omega^t} {}^{t+\Delta t}\mathbf{f}\delta\, {}^{t+\Delta t}\mathbf{u} d\Omega^t \\ + \int_{\partial\Omega^t_\sigma} {}^{t+\Delta t}\mathbf{t}\delta\, {}^{t+\Delta t}\mathbf{u} d\left(\partial\Omega^t_\sigma\right) \end{aligned} \tag{5} $$

The goal becomes one to obtain the final incremental form of the virtual work equation before discretization. Firstly, it is employed the incremental decomposition

$$ \begin{aligned} &{}^{t+\Delta t}_{t}\mathbf{E} = {}^{t}_{t}\mathbf{E} + \Delta\mathbf{E}, \quad {}^{t+\Delta t}_{t}\mathbf{S} = {}^{t}_{t}\mathbf{S} + \Delta\mathbf{S}, \quad {}^{t+\Delta t}\mathbf{u} = {}^{t}\mathbf{u} + \Delta\mathbf{u}, \\ &{}^{t+\Delta t}\mathbf{f} = {}^{t}\mathbf{f} + \Delta\mathbf{f}, \quad {}^{t+\Delta t}\mathbf{t} = {}^{t}\mathbf{t} + \Delta\mathbf{t} \end{aligned} \tag{6} $$

secondly, the following relations for stress increments

$$ {}^{t}_{t}\mathbf{S} = {}^{t}_{t}\boldsymbol{\tau}, \quad {}^{t+\Delta t}_{t}\mathbf{S} = {}^{t}_{t}\boldsymbol{\tau} + \Delta\mathbf{S} \tag{7} $$

where ${}^{t}_{t}\boldsymbol{\tau}$ is the Cauchy stress tensor and finally the strain decomposition into its linear and nonlinear parts

$$ \Delta\mathbf{E} = \Delta\mathbf{e} + \Delta\boldsymbol{\eta}, \quad \Delta\mathbf{e} = \overline{\mathbf{A}}\Delta\mathbf{u}, \quad \Delta\boldsymbol{\eta} = \frac{1}{2}\overline{\overline{\mathbf{A}}}(\Delta\mathbf{u}')\Delta\mathbf{u}' \tag{8} $$

where $\Delta\mathbf{u}'$ is the vector of the increment of the displacements derivatives with respect to Cartesian coordinates and $\overline{\mathbf{A}}$, $\overline{\overline{\mathbf{A}}}$ are the linear and nonlinear operators as follows

$$ \overline{\mathbf{A}} = \begin{bmatrix} \partial/\partial x & 0 & 0 & \partial/\partial y & \partial/\partial z & 0 \\ 0 & \partial/\partial y & 0 & \partial/\partial x & 0 & \partial/\partial z \\ 0 & 0 & \partial/\partial z & 0 & \partial/\partial x & \partial/\partial y \end{bmatrix}^T \tag{9} $$

$$\overline{\overline{\mathbf{A}}} = \begin{bmatrix} \Delta u_{,x} & 0 & 0 & \Delta v_{,x} & 0 & 0 & \Delta w_{,x} & 0 & 0 \\ 0 & \Delta u_{,y} & 0 & 0 & \Delta v_{,y} & 0 & 0 & \Delta w_{,y} & 0 \\ 0 & 0 & \Delta u_{,z} & 0 & 0 & \Delta v_{,z} & 0 & 0 & \Delta w_{,z} \\ \Delta u_{,y} & \Delta u_{,x} & 0 & \Delta v_{,y} & \Delta v_{,x} & 0 & \Delta w_{,y} & \Delta w_{,x} & 0 \\ 0 & \Delta u_{,z} & \Delta u_{,y} & 0 & \Delta v_{,z} & \Delta v_{,y} & 0 & \Delta w_{,z} & \Delta w_{,y} \\ \Delta u_{,z} & 0 & \Delta u_{,x} & \Delta v_{,z} & 0 & \Delta v_{,x} & \Delta w_{,z} & 0 & \Delta w_{,x} \end{bmatrix}$$

When substituting the relations, Eqns. (6, 7, 8) into the virtual work equation, Eqn. (5) we obtain

$$\int_{\Omega^t} \left({}_t^t\boldsymbol{\tau} \cdot \delta\boldsymbol{\eta} + \Delta\mathbf{S} \cdot \delta\Delta\mathbf{e} \right) d\Omega^t = \int_{\Omega^t} {}^{t+\Delta t}\mathbf{f}\, \delta^{t+\Delta t}\mathbf{u}\, d\Omega^t + \int_{\partial\Omega_\sigma^t} {}^{t+\Delta t}\mathbf{t}\, \delta^{t+\Delta t}\mathbf{u}\, d(\partial\Omega_\sigma^t) - \int_{\Omega^t} {}_t^t\boldsymbol{\tau} \cdot \delta\Delta\mathbf{e}\, d\Omega^t \tag{10}$$

The equation above should be solved iteratively, however, we assume that the equation is fulfilled precisely at time t and all iterations are already done. We obtain the following form of the incremental virtual work equation

$$\int_{\Omega^t} ({}_t^t\boldsymbol{\tau} \cdot \delta\boldsymbol{\eta} + \Delta\mathbf{S} \cdot \delta\Delta\mathbf{e})\, d\Omega^t = \int_{\Omega^t} \Delta\mathbf{f}\, \delta\Delta\mathbf{u}\, d\Omega^t + \int_{\partial\Omega_\sigma^t} \Delta\mathbf{t}\, \delta\Delta\mathbf{u}\, d(\partial\Omega_\sigma^t) \tag{11}$$

We employ the finite element approximation

$$\Delta\mathbf{u} = \mathbf{N}\Delta\mathbf{q}, \quad \Delta\mathbf{u}' = \mathbf{B}_L'\Delta\mathbf{q} \tag{12}$$

where $\mathbf{N}$ is the set of shape functions and $\Delta\mathbf{q}$ is the increment of nodal displacements. Let's consider the following set of equalities

$${}_t^t\boldsymbol{\tau}^{\mathrm{T}}\delta\boldsymbol{\eta} = {}_t^t\boldsymbol{\tau}\,\delta(\overline{\overline{\mathbf{A}}})\Delta\mathbf{u}' = \delta(\Delta\mathbf{u}')^{\mathrm{T}}\, {}_t^t\overline{\boldsymbol{\tau}}\,\Delta\mathbf{u}' = \delta(\Delta\mathbf{q})^{\mathrm{T}}\mathbf{B}_L' \tag{13}$$

where ${}_t^t\overline{\boldsymbol{\tau}}$ is the Cauchy matrix and $\mathbf{B}_L'$ and $\mathbf{B}_L$ are the nonlinear and linear operators.

$$\overline{\boldsymbol{\tau}} = \begin{bmatrix} {}_t^t\underline{\boldsymbol{\tau}} & & \\ & {}_t^t\underline{\boldsymbol{\tau}} & \\ & & {}_t^t\underline{\boldsymbol{\tau}} \end{bmatrix}, \quad {}_t^t\underline{\boldsymbol{\tau}} = \begin{bmatrix} {}_t^t\sigma_{xx} & {}_t^t\tau_{xy} & {}_t^t\tau_{xz} \\ & {}_t^t\sigma_{yy} & {}_t^t\tau_{yz} \\ & & {}_t^t\sigma_{zz} \end{bmatrix} \tag{14}$$

We obtain the following discretized form of the virtual work equation

$$\left(\left(\int_{\Omega^t} \mathbf{B}_L'^T\, {}_t^t\overline{\boldsymbol{\tau}}\,\mathbf{B}_L'\, d\Omega^t \right) + \int_{\Omega^t} \mathbf{B}_L^T \Delta\mathbf{S}\, d\Omega^t \right) \Delta\mathbf{q} = \int_{\Omega^t} \mathbf{N}^T \Delta\mathbf{f}\, d\Omega^t + \int_{\partial\Omega_\sigma^t} \mathbf{N}^T \Delta\mathbf{t}\, d\left(\partial\Omega_\sigma^t\right) \tag{15}$$

Now, our goal is to calculate the design derivatives of the performance functional, Eqn. 1.

Let's assume that the stresses and the displacements depend on the design variable h. Therefore, we can differentiate the equation of equilibrium with respect to the design variable h as follows

$$\int_{\Omega^t} \mathbf{B}_L^T \frac{d\Delta\mathbf{S}}{dh} d\Omega^t + \int_{\Omega^t} \mathbf{B}_L'^T \frac{d\, {}_t^t\overline{\boldsymbol{\tau}}}{dh} \mathbf{B}_L'^T\, d\Omega^t \Delta\mathbf{q} + \int_{\Omega^t} \mathbf{B}_L'^T\, {}_t^t\overline{\boldsymbol{\tau}}\,\mathbf{B}_L'\, d\Omega^t \frac{d\Delta\mathbf{q}}{dh} = \frac{d\Delta\mathbf{Q}}{dh} \tag{16}$$

The stress increment depends on the total stress at time t, strain increment and the design variable, therefore, the definition of the constitutive tangent is as follows

$$\Delta\mathbf{S} = \Delta\mathbf{S}({}_t^t\mathbf{S}, \Delta\mathbf{e}, h), \quad \frac{\partial\Delta\mathbf{S}}{\partial\Delta\mathbf{e}} = \mathbf{C}^{con}\left({}_t^t\mathbf{S}, \Delta\mathbf{e}, h\right) \tag{17}$$

Differentiating the stress increment we obtain

$$\frac{d\Delta\mathbf{S}}{dh} = \frac{\partial\Delta\mathbf{S}}{\partial\Delta\mathbf{e}}\frac{d\Delta\mathbf{e}}{dh} + \frac{\partial\Delta\mathbf{S}}{\partial\mathbf{S}}\frac{d\mathbf{S}}{dh} + \frac{\partial\Delta\mathbf{S}}{\partial h} \tag{18}$$

Employing the definition of the constitutive tensor and the finite element discretization we obtain the form of the stress increment derivative

$$\frac{d\Delta\mathbf{S}}{dh} = \mathbf{C}^{con}\mathbf{B}_L \frac{d\Delta\mathbf{q}}{dh} + \frac{d\Delta\mathbf{S}}{dh}\Big|_{\Delta\mathbf{q}(h)=const} \tag{19}$$

Substituting the stress derivative increment into the Eqn. (16) the equation for displacement design derivatives is obtained

$$\left(\int_{\Omega^t} \mathbf{B}_L^T \mathbf{C}^{con} \mathbf{B}_L + \int_{\Omega^t} \mathbf{B}_L'^T\, {}_t^t\overline{\boldsymbol{\tau}}\,\mathbf{B}_L' \right) \frac{d\Delta\mathbf{q}}{dh} = \frac{d\Delta\mathbf{Q}}{dh} - \left[\int_{\Omega^t} \mathbf{B}_L^T \frac{d\Delta\mathbf{S}}{dh} d\Omega^t \Big|_{\Delta\mathbf{q}(h)=const} + \int_{\Omega^t} \mathbf{B}_L'^T \frac{d\, {}_t^t\overline{\boldsymbol{\tau}}}{dh} \mathbf{B}_L' d\Omega^t \Delta\mathbf{q} \right] \tag{20}$$

In short, the design sensitivity equation takes the form

$$\left(\int_{\Omega^t} \mathbf{B}_L'^T\, {}_t^t\overline{\boldsymbol{\tau}}\,\mathbf{B}_L'\, d\Omega^t \right) \frac{d\Delta\mathbf{q}}{dh} + \int_{\Omega^t} \mathbf{B}_L^T \mathbf{S}\, d\Omega^t = \frac{d\Delta\mathbf{Q}}{dh} - \frac{d\Delta\mathbf{F}}{dh}\Big|_{\Delta\varepsilon=const} \tag{21}$$

On the right hand side of the Eqn. (21) we have the derivative of the loading increment with respect to the design parameter and the derivative of internal force increment with respect to the design parameter. To complete the algorithm, we need to make two steps, firstly, accumulate the displacement and the stress design derivative

$$\frac{d\, {}_t^{t+\Delta t}\mathbf{q}}{dh} = \frac{d\, {}_t^t\mathbf{q}}{dh} + \frac{d\Delta\mathbf{q}}{dh}, \quad \frac{d\, {}_t^{t+\Delta t}\mathbf{S}}{dh} = \frac{d\, {}_t^t\mathbf{S}}{dh} + \frac{d\Delta\mathbf{S}}{dh} \tag{22}$$

and secondly, calculate the derivative of the performance functional

$$\frac{d\, {}_t^{t+\Delta t}\Phi}{dh} = \int_{\Omega^t} \left[\frac{\partial\, {}_t^{t+\Delta t}G}{\partial\, {}_t^t\mathbf{S}} \frac{d\mathbf{S}}{dh} + \frac{\partial\, {}_t^{t+\Delta t}G}{\partial\mathbf{q}} \frac{d\mathbf{q}}{dh} + \frac{\partial\, {}_t^{t+\Delta t}G}{\partial h} \right] d\Omega^t + \int_{\partial\Omega_\sigma^t} \frac{\partial\, {}_t^{t+\Delta t}g}{\partial\mathbf{q}} \frac{d\mathbf{q}}{dh} d\left(\partial\Omega_\sigma^t\right) + \int_{\partial\Omega_\sigma^t} \frac{\partial\, {}_t^{t+\Delta t}g}{\partial h} d\left(\partial\Omega_\sigma^t\right) \tag{23}$$

The constitutive model is visco-elastic such as the stress increment depends on total stress $\mathbf{S}$, the shear modulus (G), the bulk modulus (K) and the strain increment $\Delta\mathbf{E}$ as follows

$$\Delta\mathbf{S} = \mathbf{C}^{con}(\mathbf{S}, \mathbf{G}, \mathbf{K})\Delta\mathbf{E}\,, \; G(t) = G_o + \sum_{i=1}^{n} G_i \exp\left(\frac{t}{\lambda_i}\right) \tag{24}$$

where t is the time and λ_i are the relaxation times of the particular parallel dampers. The Eqns. (24) describe the generalized Maxwell model.

4. Numerical aspects

The parallel version of the program includes the solver MUltifrontal Massively Parallel Solver, MUMPS [2, 3]. We use the Newton-Raphson technique for solving the equation of equilibrium, Eqn. (15). The sensitivity algorithm creates additional right hand sides, Eqn. (21). We need to solve so many right hand sides as the design variables. The design sensitivity equation is solved using the triangularized form of the last stiffness obtained in the last iteration loop.

5. Numerical examples

5.1. Scratch appearance

We consider a honeycomb pattern of the single layer cell matrix, Fig. 4.

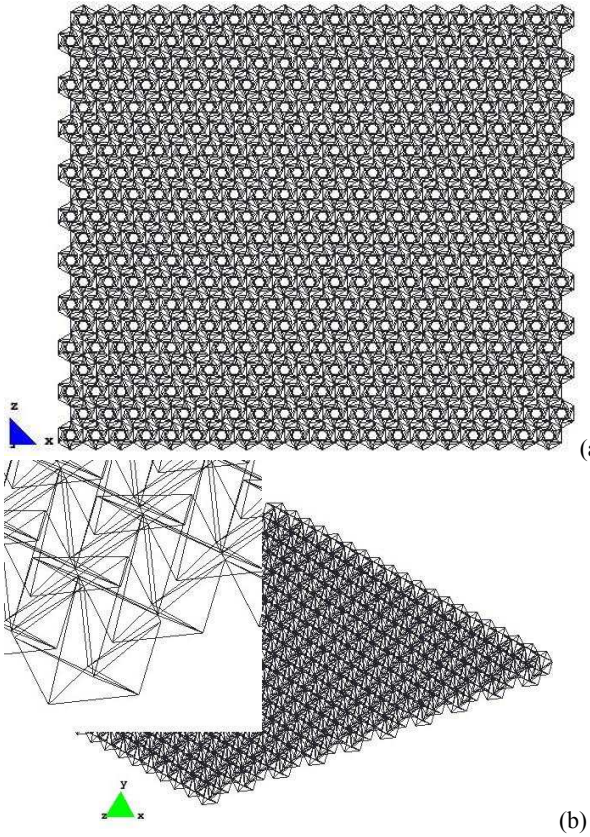

(a)

(b)

Figure 4: Matrix of elementary cells: a) top view b) axonometry and a corner detail.

We are assuming the same data for each single cell as in the Section 2. The layer of cells can slide and is fixed on its right side preventing rigid body motions, Fig. 4. It is loaded with the concentrated forces on the left side, each concentrate force is 100.0d-04N. We will assume that the tissue is scratched after 0.1 sec of the loading process. We will observe the sensitivity fields of the displacements with respect to the design variables such as: we have 3 cells in which all microtubules can change simultaneously their lengths. The displacement field and the design sensitivity field are shown in Fig. 5. The displacement sensitivity field is shown in Fig. 6.

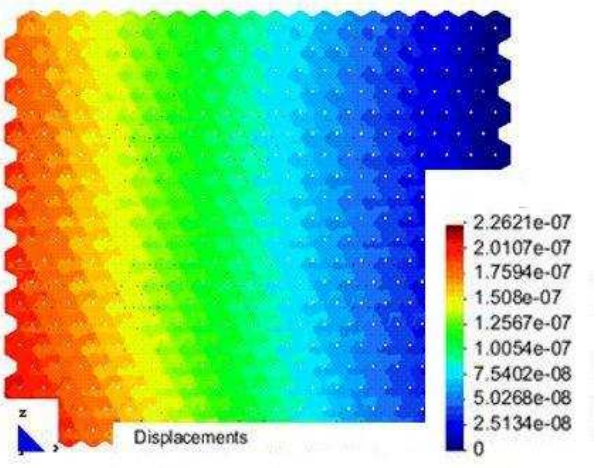

Figure 5: Beginning of the process, displacements field.

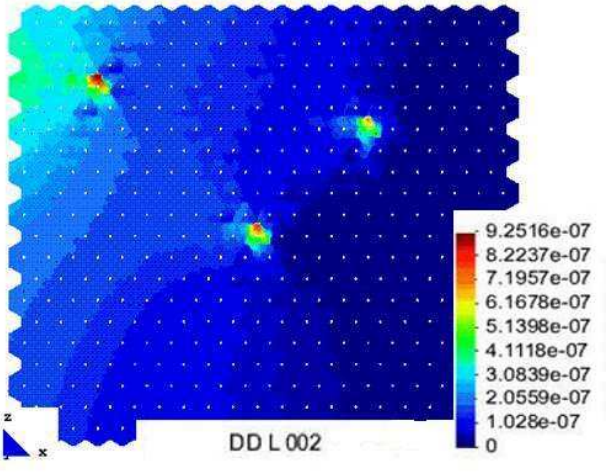

Figure 6: Beginning of the process, design sensitivity field

We may note that the most sensitive places in the layer are in the neighbourhood of the supposed to be perturbed cells. The sensitivities of the system are shown at the beginning of the scratch appearance, Fig. 7(a) and at the end of its development, Fig. 7(b).

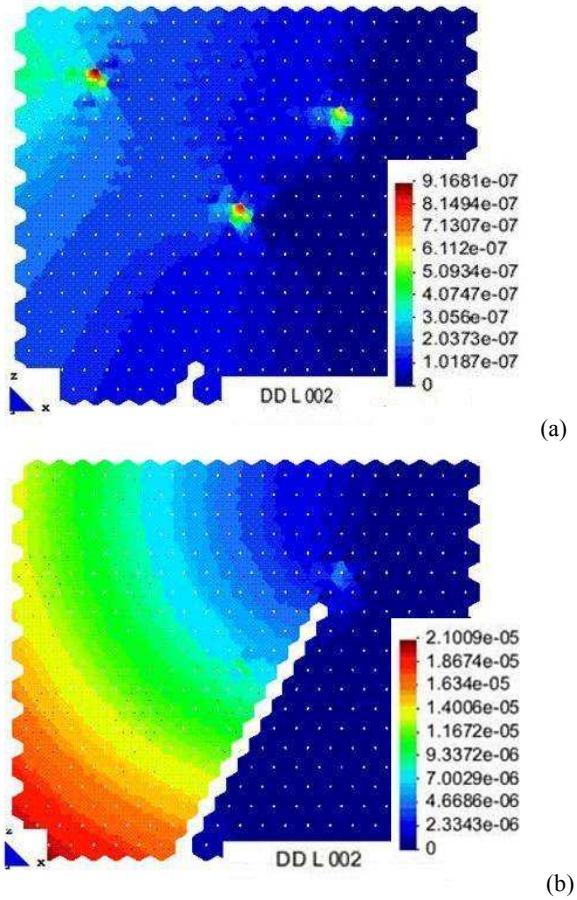

(a)

(b)

Figure 7: Process development; a) beginning of scratch appearance, b) end of the process

We observe that at the beginning of the scratch appearance the most sensitive places are again in the neighbourhood of the chosen cells. However, the picture becomes different at the end of the process. The DSA gradients are becoming regularly

distributed on left side of the scratch. It means that the chosen cells have stopped to be the most important. The perturbation of the design parameters in the chosen cells makes similar effects in entire structure on left side and the gradients are of range higher. This means that the structure approaches failure.

5.2. Holes and slits

Let us consider a tissue made of 10000 elementary cells. We will observe the sensitivities and we will demonstrate that the model can catch the effect of the stress concentrations.

The boundary conditions and the loading are the same as in the structure presented above. We will consider the tissue with a punched hole and a slit. The displacement fields are shown in Fig. 6.

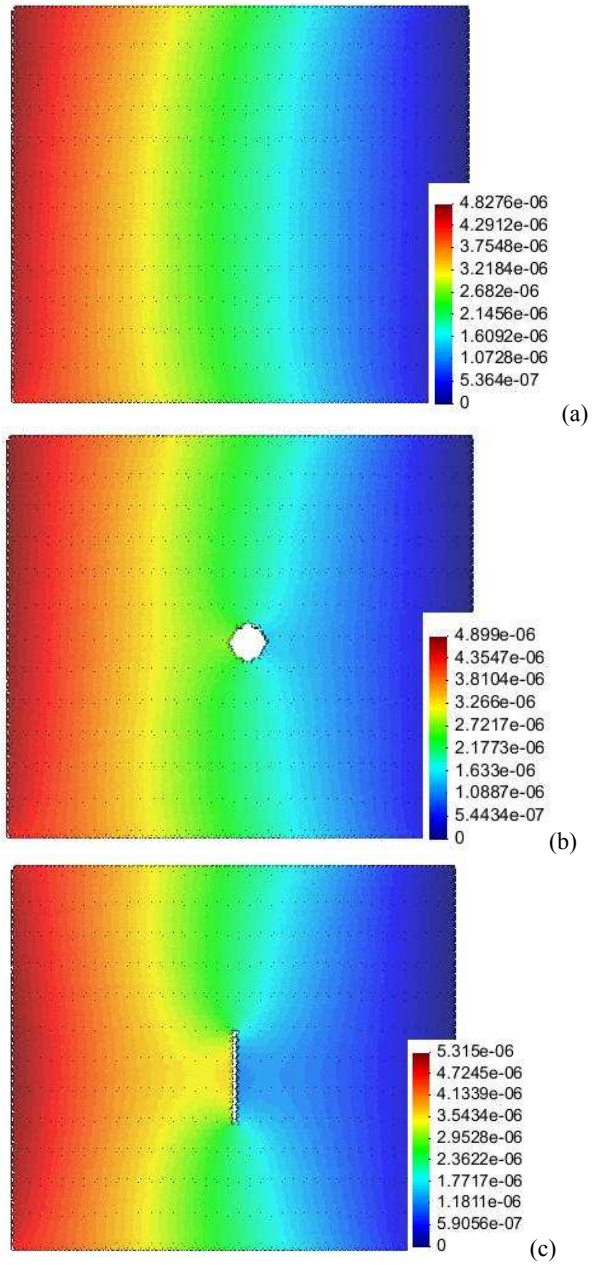

Figure 6: Displacement fields; a) ideal tissue, b) hole, c) slit

We observe that the displacement fields are perturbed around the openings what demonstrates the applicability of the model and the reticular medium to describe the continuous tissue.

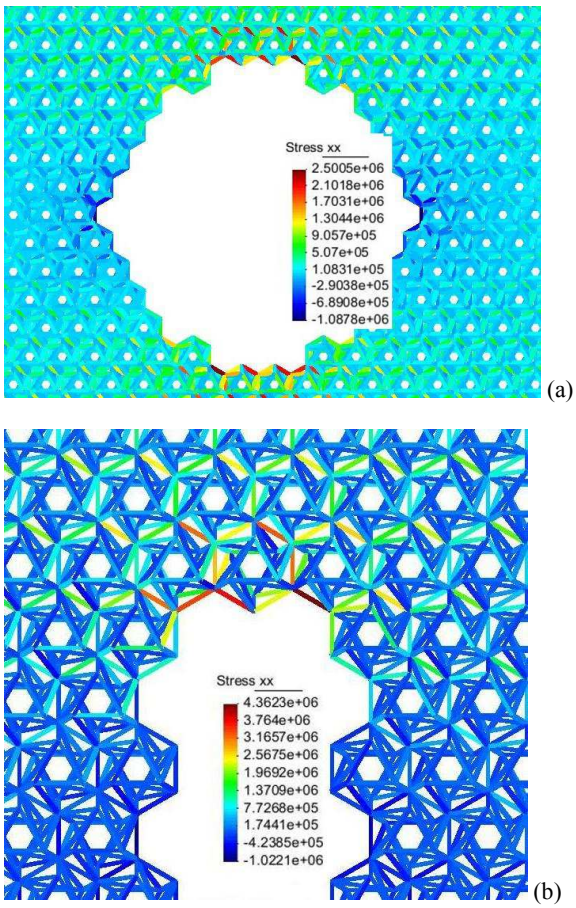

Figure 7: Stress concentrations a) hole b) slit

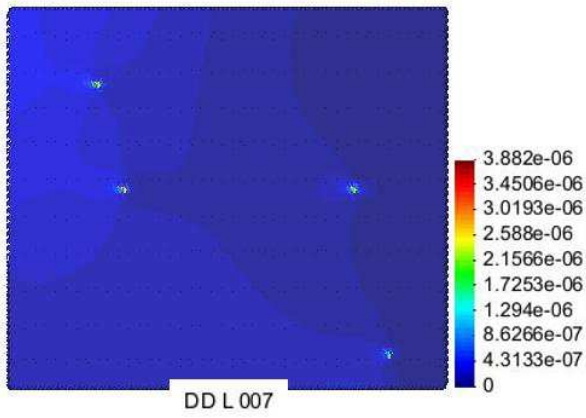

Figure 8: Design sensitivity field, ideal system

The stress concentrations in the hole and the slit are shown in Fig. 7. The stresses are significantly higher at the tip of the slit than around the hole.

The considered design sensitivity fields are shown in Fig. 8. The design variables are defined as the sum of the lengths of the microtubules in 4 cells. The cells are easily visible in Fig. 8.

When comparing the maximum sensitivities we note that the less sensitive to the defined set of the design parameters is

the ideal system (Fig. 8) and the most sensitive is the system with the slit (Fig. 10). The system with the slit is moderately sensitive, Fig. 9.

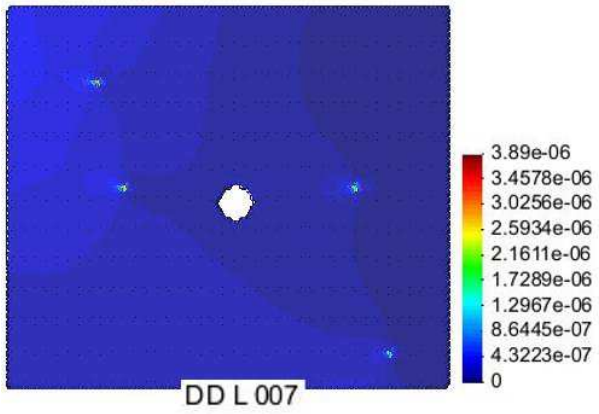

Figure 9: Design sensitivity field, hole

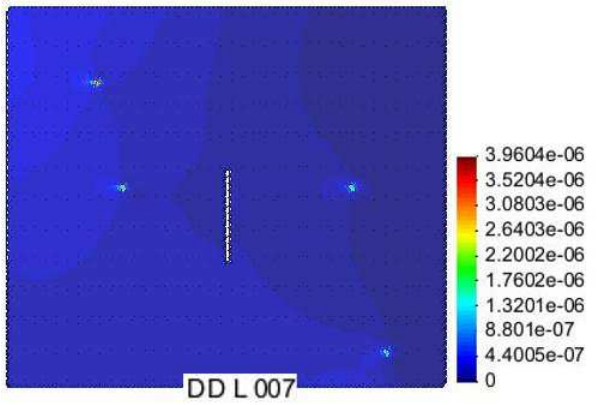

Figure 10: Design sensitivity field, slit

6. Final remarks

We have presented the implemented design sensitivity algorithm valid for nonlinear path dependent systems. The application of it is the computational systems biology. We have described numerical aspects of the implementation with parallel multifrontal solver. We have shown a numerical example and possible scenarios of application of the presented theory. The resulting computer program will serve as a physical solver of an agent based system, Ref [7].

References

[1] Ainsworth C., Stretching the imagination, *Nature*, 456, 1 Dec, pp. 696-699, 2008.

[2] Amestoy P.R, Duff I.S., Koster J. and L'Excellent J.-Y., A fully asynchronous multifrontal solver using distributed dynamic scheduling, *SIAM Journal of Matrix Analysis and Applications,* 23, 1, pp 15-41, 2001.

[3] Amestoy, P.R., Guermouche A., L'Excellent J.Y. and Pralet S. (2006) Hybrid scheduling for the parallel solution of linear systems. *Parallel Computing*, 32, 2, pp 136-156, 2006.

[4] Kleiber M., Antunez H., Hien T.D., Kowalczyk P. *Parameter Sensitivity in Nonlinear Mechanics: Theory and Finite Elements*, Wiley & Sons, 1997.

[5] Malvern L.E., *Introduction to the continuum mechanics*, PWN – Englewood Cliffs, 1989.

[6] Postek E.W., Smallwood R. And Hose R., Nodal positions displacement sensitivity of an elementary icosahedron tensegrity structure, X *Int. Conference on Computational Plasticity,* COMPLAS X, Barcelona, Spain, September, 2009.

[7] Postek E., Concept of an agent-stress model of a tissue, accepted to 2nd *Int. Conference on Material Modelling, Paris,* France, September 2011.

[8] Stamenovic D., Effects of cytoskeletal prestress on cell rheological behaviour, **1**, *Acta Biomaterialia*, pp. 255-262. 2005.

[9] Walker D, Wood S, Southgate J, Holcombe M, Smallwood R., An integrated agent-mathematical model of the effect of intercellular signalling via the epidermal growth factor receptor on cell proliferation. *J Theor. Biol*. 242, pp. 774-789, 2006.